Solid State Science and Technology, Vol. 29, No 1 & 2 (2021) 11-21
ISSN 0128-7389 | *http://myjms.mohe.gov.my/index.php/masshp*

CATION/ANION SUBSTITUTION INTO SPINEL $LiMn_2O_4$ CATHODE MATERIAL FOR LI-ION BATTERY APPLICATION: A REVIEW OF RECENT PROGRESS

Z. Ahmed[1,2*], J.Y.C. Liew[1] and Z. A. Talib[3,4]

[1] *Department of Physics, University Putra Malaysia, 43400 UPM, Sedang, Selangor Malaysia*

[2]*Discipline of Chemistry, The University of Newcastle Callaghan, NSW 2308, Australia*

[3]*Department of Physics, College of Natural Sciences, Jeonbuk National University, Baekje-daero, Deokjin-gu, Jeonju-si, Jeollabuk-do, 54896 Republic of Korea*

[4]*RGS Corporation Sdn Bhd, SB15, Serdang Skyvillas Jalan SP 5/5, 43300 Seri Kembangan, Selangor, Malaysia*

**Corresponding author: zahoor.ahmed@uon.edu.au*

Received: 10 November 2021
Accepted: 16 December 2021

ABSTRACT

Spinel $LiMn_2O_4$ is a positive electrode material with a robust structure. It has a three-dimensional network of channels for fast lithium-ion diffusion in state-of-the-art lithium rechargeable batteries. It is commercialized because of its high-power and cost-effective natural abundant element. However, its capacity fading and cycle performance, originating from Mn dissolution, still need improvement. In this review, the recent development of the effect of cation and anion doped into the spinel $LiMn_2O_4$ cathode material is thoroughly investigated. The effect of anion substitution on the morphology and electrochemical properties were investigated. Cation/anion substitution shows improvement in the structural stability and suppresses lattice deformation of the material. Finally, some insight into the future prospects for spinel cathode developments is provided.

INTRODUCTION

Lithium-ion batteries (LIBs) are state-of-the-art technology in today's world and are used in devices such as computers[1], smart phones[2], grid stabilization[3], electric vehicles, and plug-in hybrid electric vehicles[4] owing to their high power and energy density as well as their long cycle life and flat discharge voltage[5]. Significant advancements in application and commercialization have been made in the field of lithium-ion batteries (LIBs) over the last 20 years[6]. However, due to increasing power and energy demands on batteries, next-generation batteries[7] will require further

improvements in cycle life, energy density, and power density. As such, worldwide research on the design of promising cathode material for lithium-ion batteries (LIBs) will overcome the rising energy market demand for better security, and cost is ongoing[8-10]. Among all existing cathode materials such as $LiFePO_4$ and $LiCO_2$, spinel $LiMn_2O_4$ with 3D lithium-ion diffusion paths and its derivatives has emerged as an exciting material by natural abundance, environmental friendliness, low toxicity, low-cost, high operating plateaus, and high specific capacity[11,12].

Nevertheless, spinel also suffers from capacity fading[13] due to the dissolution of manganese ions and poor high rate capability due to Jahn-Teller distortion[14-15]. Various strategies to mitigate the effect of Jahn-Teller distortion have been employed, including the substitution of Mn with other cations, such as Li^+ [16], Ni^{2+} [17], Mg^{2+} [18], Zn^{2+} [19], Al^{3+}[20], Cr^{3+} [21], Co^{3+} [22], and Ti^{+4} [23]. Further, the anionic substitution of fluorine with oxygen forming spinel oxyfluorides can reduce the overall Mn oxidation state and improve the chemical and structural stability of the spinel[24-26]. J. T. Son et al. [27] reported that the substitution of fluorine for O_2 in the single-phase region improved the initial discharge capacity of the spinel $LiMn_2O_4$. However, they also showed that the cycle performance was reduced considerably compared with that of parent $LiMn_2O_4$. He et al. [28] reported that surface fluorine doping of the lithium-rich spinel $Li_{1.15}Mn_{1.85}O_4$ showed a high cycling efficiency. Similar results were seen by Yonezawa et al. [29] for surface fluorine coating of spinel $LiMn_2O_4$ with an increased initial discharge capacity of 6% more than the $LiMn_2O_4$. Furthermore, W. Wen et al. [30] studied the effect of Mg and F doping on the structure and electrochemical performance of the spinel $LiMn_2O_4$. These authors showed that $LiMg_{0.1}Mn_{1.9}O_{3.8}F_{0.2}$ exhibits a much higher discharge capacity of 121.4 mAh g^{-1} at a rate of 1 C with excellent capacity retention of 96.0% after 400 cycles at room temperature, as a comparison to pristine $LiMn_2O_4$ with 117.2 mAh g^{-1} discharge capacity and 79% capacity retention. Toyoki and Choi et al. [31] used a low-temperature doping approach with NH_4F or NH_4HF_2 as a precursor as a successful synthesis of series of fluorinated spinel-type $LiMn_{1.8}Li_{0.1}Ni_{0.1}F_x$ (x = 0,00.018, 0.036, 0.0055, 0.073, 0.11, 0.180) at a low temperature 450 °C by reaction between spinel and NH_4HF_2 [32]. Their research concluded that the fluorination of these spinels enhanced cyclability compared to a pristine spinel. However, there are some reports on the fluorinated spinels $LiNi_{0.5}Mn_{1.5}O_4$ at high temperature that ranges between 700 °C-900 °C[33,34] that shows the excellent electrochemical performance of the cathode material as a comparison to other low-temperature spinels.

This review aims to highlight the recent progress from 2011- 2021 and looks forward to the prospects of cation/anion doped $LiMn_2O_4$ spinel cathode materials for lithium-ion batteries (LIBs). First, a brief review of the synthesis, morphological and electrochemical diagnostics during cell operation for these spinels is presented. To be concise, only a limited number of references have been selected for this review paper. The papers selected in this review are based on characterization methods like solid-state, their scanning electron microscopy for morphological understanding, and finally, electrochemical analysis to overview the best performance cation/anion doped spinel materials.

EXPERIMENTAL

Synthesis, Morphology and Electrochemical Performance of spinel $LiMn_2O_4$
The flow chart of this review work is shown in Figure 1.

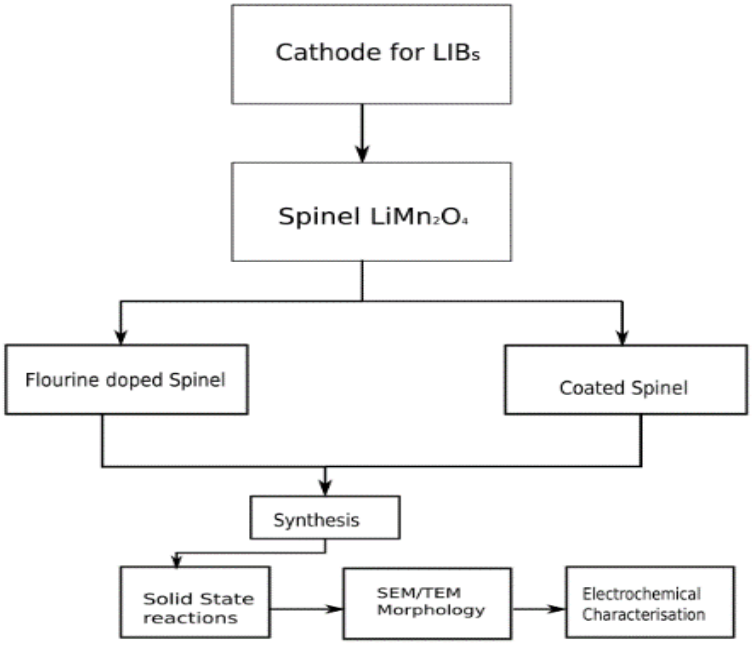

Figure 1: Flow chart of the review work

Table 1: Comparison of various cathodes for lithium-ion batteries (LIBs)

Cathode Materials vs Li/Li^+	Calculated Capacity (mAh g^{-1})	Experimental Capacity (mAh g^{-1}) @ C/10	Energy Density (Wh kg^{-1})	Operating Voltage (V)	References
$LiMn_2O_4$	148	120	490	4.1	[9]
NMC811	276	205	780	3.8	[9]
$LiMn_{1.5}Ni_{0.5}O_4$	147	125	590	4.7	[9]
$LiMn_{1.5}Cr_{0.5}O_4$	149	80	590	4.8	[21]
$LiMnCoO_4$	147	85	590	5	[22]

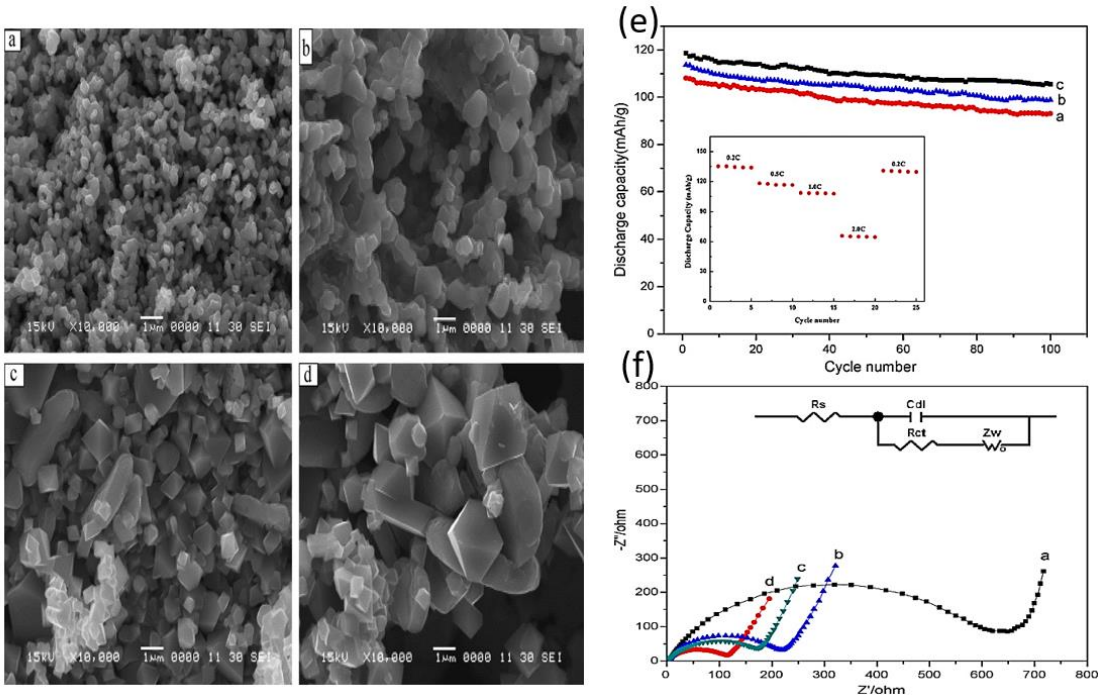

Figure 2: SEM micrographs of (a) $LiMn_2O_4$, (b) $Li_{1.02}Mn_{1.95}Co_{0.02}Y_{0.01}O_4$, (c) $Li_{1.02}Mn_{1.95}Co_{0.02}Y_{0.01}Ga_{0.01}O_4$, and (d) $Li_{1.02}Mn_{1.95}Co_{0.02}Y_{0.01}Ga_{0.01}O_{3.97}F_{0.03}$ (e) Discharge capacity vs cycle number at a current density of 0.5 C. Inset shows the C-rates of the $Li_{1.02}Mn_{1.95}Co_{0.02}Y_{0.01}Ga_{0.01}O_{3.97}F_{0.03}$ electrode at various C-rates. (f) EIS of the samples. Inset shows the Randles equivalent circuit for the electrode/electrolyte interface. Re is the electrolyte resistance, and Cdl and Rct are the double-layer capacitance and charge-transfer resistance, Zw is the Warburg impedance respectively. Source: Reproduced from Ref. [35]

Feng et al. [35] reported four spinel compounds ($LiMn_2O_4$, $Li_{1.02}Mn_{1.95}Co_{0.02}Y_{0.01}O_4$, $Li_{1.02}Mn_{1.95}Co_{0.02}Y_{0.01}Ga_{0.01}O_4$, and $Li_{1.02}Mn_{1.95}Co_{0.02}Y_{0.01}Ga_{0.01}O_{3.97}F_{0.03}$) that were synthesized by rheological phase reaction method. Their samples were obtained by the two-step sintering method, in which the precursor was heated at 550 °C for six h and then was ground to a fine powder and calcined at 820 °C in air for ten h. As it can be seen clearly in Figure 2(b)–(d), the doped sample particles have an octahedral shape. By comparing Figure 2(b)–(d) with Figure 2(a), it can be seen that the substituted samples have a slightly larger particle size than the undoped $LiMn_2O_4$, and this is particularly true for the sample in Figure 2(d), which is doped with fluorine and takes on a clear octahedral particle shape. The galvanostatic charge-discharge (GCD) cycling of the substituted samples at a current density of 0.5 C at 25 °C are shown in Figure 2(e). By increasing C-rates, the initial discharge capacities of substituted samples reduce to 108, 113, and 118 mAh g^{-1}, respectively. After 100 cycles, the capacity retention is at 93, 99, and 105 mAh g^{-1}, respectively. However, the discharge capacities decrease with increasing current density, the $Li_{1.02}Mn_{1.95}Co_{0.02}Y_{0.01}Ga_{0.01}O_{3.97}F_{0.03}$ sample still shows

higher discharge capacity and better cycling performance compared with the other substituted samples. Apparently, the cathode displays good capacity retention at different C-rates. When the current rates are 0.2, 0.5, 1, and 2 ◦C, the specific capacities are 131, 118, 106, and 65 mAh g^{-1}, respectively. Electrochemical impedance spectroscopy (EIS) was performed to understand the impedance measurements of the samples. Figure 2(f) shows that the impedance of the substituted samples is lower in comparison with the undoped $LiMn_2O_4$, which shows that the doped samples have fewer charge transfer impedances. Figure 2 illustrates that substituted spinels had slightly larger particle sizes and more regular morphology than undoped $LiMn_2O_4$. Electrochemical measurements of the as-prepared samples have proved that the substituted spinels have more stable cycling performance than $LiMn_2O_4$.

Wang et al. [36] reported $LiMn_2O_4$, Al-doped $LiMn_2O_4$, F-doped $LiMn_2O_4$, and Al, F co-doped $LiMn_2O_4$ was prepared by a two-step heating method at 560 °C for 10 h and then annealed at 800 °C for 20 h in air. Finally, for AlF_3 coating, $LiMn_{1.96}Al_{0.04}O3.94F_{0.06}$ samples were sintered at 400 °C for five h/N_2. Figures 3(a)-(b) exhibit the morphologies of the $MnCO_3$ precursors and $LiMn_2O_4$. Figure 3(c)–(e) shows bare, doped, and doped-coated $LiMn_2O_4$ samples. Moreover, it is evident that F doped $LiMn_2O_4$ (Figure 3(d)) and co-doped $LiMn_2O_4$ (Figure 3(e)) display microporous structures having larger primary particles. The electrochemical performance of these materials at 55 °C, Figure 3(g)-(a) displays the 1st galvanostatic charge-discharge (GCD) profiles of the pristine and AlF3-coated sample at a rate of C/2. It was evident that AlF3-coated shows higher discharge capacity as a comparison to pristine spinel. To further examine the surface coating effect, the differential capacity dQ/dV vs. voltage curves of the pristine and AlF3-coated is shown in Figure 3(g)-(b). In Figure 3(g)-(c), the pristine and AlF3-coated exhibit similar initial discharge capacity of 109 mAh g^{-1} after 100 cycles at room temperature 25 °C, but AlF3-coated reveals a higher capacity at 55 °C after 50 cycles as a comparison to pristine spinel. Conclusively, the AlF3 coating layer could prevent remarkably improving the cycling performance at high temperature 55 °C. EIS measurements for 1st and 100th cycles indicate that doping with surface modification is an effective method to improve the electrochemical performance of spinel $LiMn_2O_4$ at elevated temperature as shown in Figure 3(h)-(a) and (h)-(b).

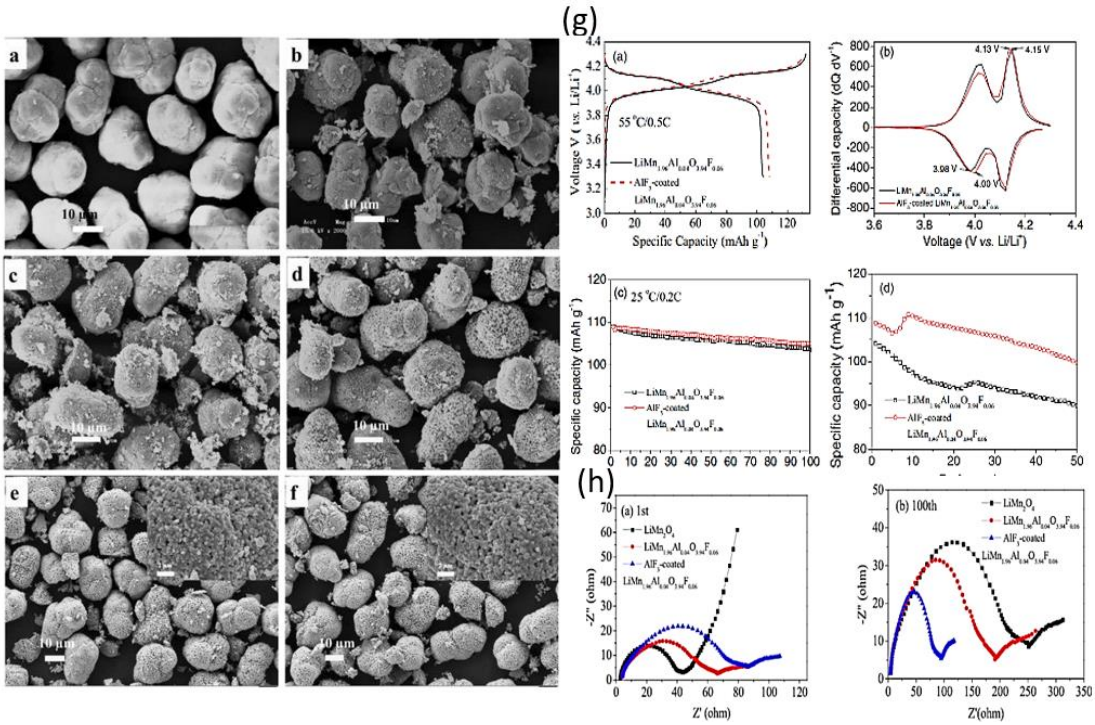

Figure 3: SEM images: a. $MnCO_3$, b. $LiMn_2O_4$, c. $LiMn_{1.96}Al_{0.04}O_4$, d. $LiMn_2O_{3.94}F_{0.06}$, e. low and high magnification of $LiMn_{1.96}Al_{0.04}O_{3.94}F_{0.06}$, and f. AlF_3-coated $LiMn_{1.96}Al_{0.04}O_{3.94}F_{0.06}$. (g)-(a) The first charging and discharging curves of the bare and AlF_3-coated $LiMn_{1.96}Al_{0.04}O_{3.94}F_{0.06}$ between 3.3 and 4.3 Vat 0.5C (55 °C). (g)-(b) dQ/dV vs. voltage curves of the pristine and AlF_3-coated $LiMn_{1.96}Al_{0.04}O_{3.94}F_{0.06}$ electrodes during the first cycle. (g)-(c) Cycle performance of AlF_3- coated $LiMn_{1.96}Al_{0.04}O_{3.94}F_{0.06}$ between 3.3 and 4.3 V at 25 °C and (g)-(d) at 55 °C. EIS of $LiMn_2O_4$, $LiMn_{1.96}Al_{0.04}O_{3.94}F_{0.06}$, and AlF_3-coated $LiMn_{1.96}Al_{0.04}O_{3.94}F_{0.06}$ at the 1st cycle (h)-(a) and 100th cycle (h)-(b) and their equivalent circuit model (c), where Rs and Rct represent solution resistance and charge transfer resistance, respectively (d) The relationship between Zw and $\omega^{-1/2}$ at low frequency. The capacity of $LiMn_2O_4$, $LiMn_{1.96}Al_{0.04}O_{3.94}F_{0.06}$, and AlF_3-coated $LiMn_{1.96}Al_{0.04}O_{3.94}F_{0.06}$ is 106, 104, and 105 mAh g^{-1}, respectively [36]

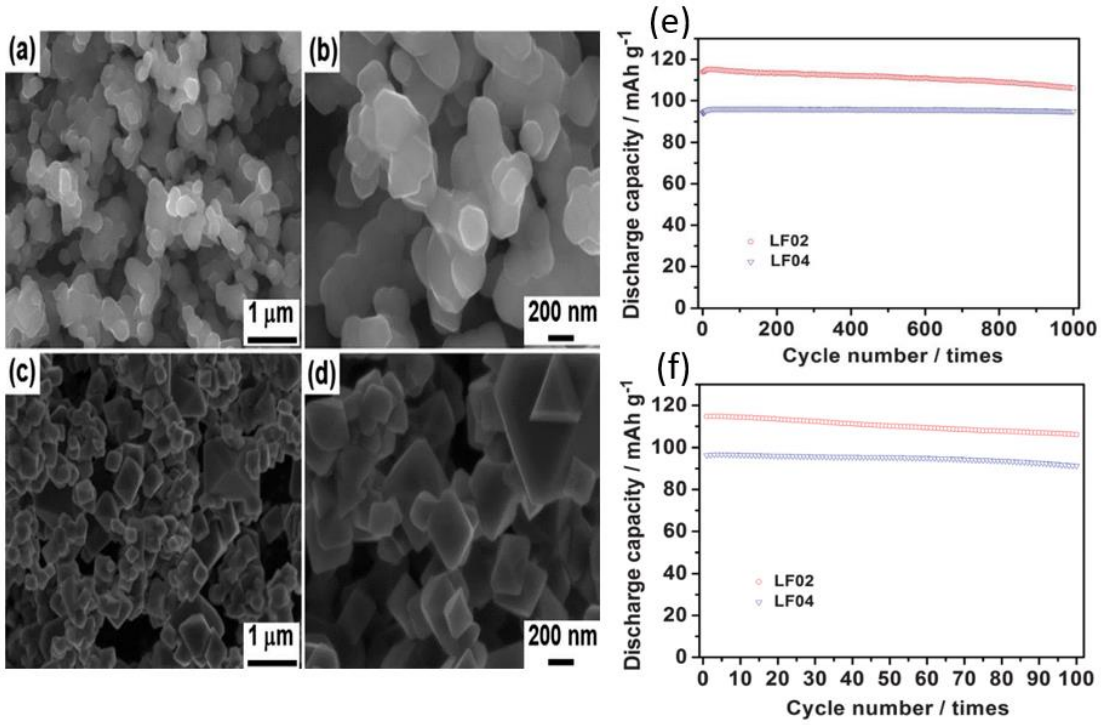

Figure 4: SEM micrographs for the samples: (a) LF0 at low magnification, (b) LF0 at high magnification, (c) LF04 at low magnification, (d) LF04 at high magnification. (e) The cycling performance of LF02, LF04 samples cycled at 1 C at room temperature. (f) The cycling performance of the LF02 and LF04 samples cycled at C/2 at 55 °C. Both the samples display capacity-retention at 55 °C elevated temperature [37]

Xiong et al. [37] reported $LiMn_2O_4$ based composites having LiF as the dopant and Li_2MnO_3 thin surface coating prepared by one-step solid-state reaction method for 48 h followed by sintering at 450 °C for six h and then final calcination at 750 °C for 12 h. The values of the molar concentration of LiF were 0, 0.2, 0.4, 0.6, and the corresponding samples were marked as LF0, LF02, LF04, LF06, respectively. Figure 4(a-d) displays the SEM of the particles of the LF0 sample with a size of 200 nm exhibit good crystallinity, while the particles of the LF04 sample show much more prominent grown facets with a defined grain boundary. They reported the long-term stability of the doped spinel LF02 and LF04 samples are tested at 1 C at 25°C for 1000 cycles, as shown in Figure 4(e). The results show that both LF02 and LF04 samples could deliver a discharge capacity of 106 and 94.9 mAh g^{-1}, and the corresponding capacity retention is 92% and 98.8% after 1000 cycles. Figure 4(f) shows the cycling performance at elevated temperature 55 °C at a rate of C/2 for both doped samples. Therefore, the capacity retention ratio for both samples LF02 and LF04 were 92.3% and 94.3%, respectively, after 100 cycles. The results indicate that the modification of Li and F doping and surface coating of Li_2MnO_3 could effectively improve the cyclic performance as well high-temperature stability of spinel as cathode material for LIBs.

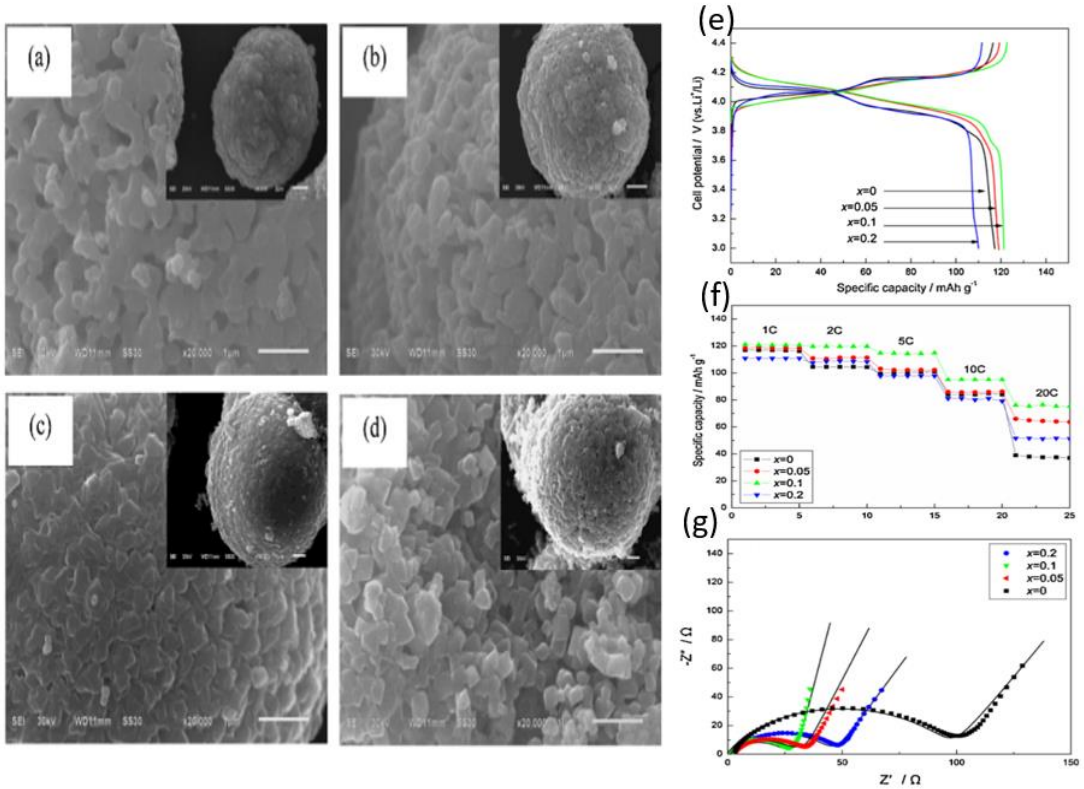

Figure 5: SEM images of high magnification of the $LiMg_xMn_{2-x}O_{4-2x}F_{2x}$ (x= 0, 0.05, 0.1, 0.2). (a) x= 0; (b) x= 0.05; (c) x= 0.1; (d) x= 0.2. The insets are the relative low magnification of the $LiMg_xMn_{2-x}O_{4-2x}F_{2x.}$ (e) initial charge-discharge curves of the samples at 1 C in the voltage range of 3.0–4.4 V. (f) The C-rate performance of the samples in the voltage range of 3.0–4.4 V (g) Nyquist plots of the all the samples [38]

Wen et al. [30] reported $LiMg_xMn_{2-x}O_{4-2x}F_{2x}$(x = 0, 0.05, 0.1, 0.2) samples prepared by solid-state reaction method having MgF_2 as the dopant. First, $MnCO_3$ was sintered at 560 °C for 6 h, the final mixture containing Li carbonates, Mn oxides, and MgF_2 was sintered at 750 °C for 20 h. The SEM images of F doped spinel samples are shown in Figure 5. The morphology shows increasing the fluorine molar ratio from 0 to 0.2 the geometry of the primary particles varies from irregular shape to regular cubic octahedral crystallite. It is suggested that F ions are successfully substituted into the host spinel structure. The electrochemical performance of the doped spinels samples was measured by galvanostatic charge-discharge curves at 1 C, as shown in Figure 5 (e). The samples with F=0.1, 0.2 and Mg= 0.05, 0.1 molar ratio deliver the highest discharge capacity of 119.1 mAh $g^{-1}$and 121.4 mAh g^{-1}, compared to the pristine spinel $LiMn_2O_4$ having 117.2 mAh g^{-1}. C-rates were also studied in their research work for further comparison and stability of the samples of the substituted spinels, as shown in Figure 5(f). All the samples were charged at the same rate of C/2 and then discharged at various C-rates from 1 to 20 C. The doped samples having x= 0.1 present the best rate capability among all the samples. It delivers the highest discharge capacity of 121.1, 119.7, 114.7, 95.0, 76.1 mAh g^{-1} at C-rates of 1C, 2C, 5C, 10C, and 20C, respectively. Therefore, it can be possible that both Mg and F substitution will result in a larger cell volume, which

enables Li-ion intercalation/de-intercalation, especially at high C-rates. EIS measurements were also also carried out in order to understand the doped samples impedance and conductance properties as shown in Figure 5(g). The charge transfer resistance of the Mg-F substitution samples are much less than one of the pristine spinel $LiMn_2O_4$ sample, showing that the electrochemical reaction resistance is drastically reduced by the dopant. Therefore, the small charge transfer resistance is favourable to the rapid electrochemical reaction and may result in better electrochemical performance of the cathode material.

Li et al. [38] reported $LiMn_2O_4$ based composites having Al-F as the dopant prepared by solid-state reaction method at a calcination temperature of 780 °C for 15 h. They reported that SEM reveals that the sample is single-crystal Li1.05Al0.02Mn1.98F0.02O3.98 with uniform grain distribution and regular morphology. This sample has excellent cycle performance, and its initial discharge specific capacity is 115.5 mAh g^{-1} at C/10. Furthermore, the capacity retention rate is still above 80% after 367 cycles, and the specific capacity is 90.3 mAh g^{-1}. The Al-F co-doping modified spinel material can effectively hinder the Jahn-Teller effect and increase the Li-ions diffusion channel, thus stabilizing the crystal structure of the material, and this in return improves the cyclic performance of the battery cathode material.

CONCLUSIONS

To conclude, the synthesis and electrochemical characterization of spinel $LiMn_2O_4$ cathode and its dopants were reviewed in this study, which provides valuable insights for the future development of LIBs cathodes material. There are several advantages of these dopant spinels in terms of low cost, environmentally friendly, good thermal stability, good conductivity, high rate stability, and simple synthesis, the doped spinel cathodes such as $LiMn_2O_4$, $LiM_xMn_{2-x}O_{4-2x}F_{2x}$(M= Mg, Al, Co, Ga, Y x = 0, 0.05, 0.1, 0.2) are promising cathode material for next generation of LIBs. So far, there has been a tremendous amount of success achieved in commercializing these spinel cathode materials. Moreover, various approaches are used to improve the cycle and c-rates performance of spinel cathode material. Therefore, these methods include solid-state reaction, surface, cation/anion doping. Furthermore, it is believed the following aspects are of central importance in spinel cathodes:

1) There is a need for more basic synthesis studies such as solvothermal and hydrothermal methodologies should be deployed better to understand the poor cycling of spinel cathodes materials;
2) There must be special care taken for surface doping and development of new solid-state electrolytes for future solid-state lithium-ion battery applications;
3) Advanced machine learning and data-driven models should be tested in understanding various dopants and exploring new cathode materials.

ACKNOWLEDGEMENTS

The University of Newcastle is acknowledged for the 2016 International Tuition Fees

Scholarship and 2017 UNRS Central Scholarship. Finally, we also recognize the support from University Putra Malaysia on the joint degree program.

REFERENCES

[1] Horiba, T. *Proceedings of the IEEE*, **102**(6) 939-950 (2014)
[2] Pistoia, G. (Ed.). *Lithium-ion batteries: advances and applications*. Newnes. (2013)
[3] Yoshino, A. Development of the lithium-ion battery and recent technological trends. In *Lithium-ion batteries* (pp. 1-20). Elsevier. (2014)
[4] Hannan, M. A., Lipu, M. H., Hussain, A., & Mohamed, A. *Renewable and Sustainable Energy Reviews*, **78** 834-854 (2017)
[5] Yang, M., & Hou, J. *Membranes*, **2**(3) 367-383(2012)
[6] Bensalah, N., & Dawood, H. (2016). Review on synthesis, characterizations, and electrochemical properties of cathode materials for lithium ion batteries.
[7] Huggins, R. *Advanced batteries: materials science aspects*. Springer Science & Business Media. (2008)
[8] Goodenough, J. B., & Kim, Y. *Chemistry of materials*, **22**(3) 587-603 (2010)
[9] Huang, Y., Dong, Y., Li, S., Lee, J., Wang, C., Zhu, Z., ... & Li, J. *Advanced Energy Materials*, **11**(2) 2000997 (2021)
[10] Etacheri, V., Marom, R., Elazari, R., Salitra, G., & Aurbach, D. *Energy & Environmental Science*, **4**(9) 3243-3262 (2011)
[11] Mao, F., Guo, W., & Ma, J. *RSC advances*, ***5***(127) 105248-105258 (2015)
[12] Xiong, L., Xu, Y., Tao, T., Song, J., & Goodenough, J. B. *Journal of Materials Chemistry*, **22**(47) 24563-24568 (2012)
[13] Zhuo, Z., Olalde-Velasco, P., Chin, T., Battaglia, V., Harris, S. J., Pan, F., & Yang, W. *Applied Physics Letters*, ***110***(9), 093902 (2017)
[14] Zhan, C., Wu, T., Lu, J., & Amine, K. *Energy & Environmental Science*, ***11***(2), 243-257 (2018)
[15] Park, O. K., Cho, Y., Lee, S., Yoo, H. C., Song, H. K., & Cho, J. *Energy & Environmental Science*, ***4***(5), 1621-1633 (2011)
[16] Gao, Y., & Dahn, J. R. *Journal of the Electrochemical Society*, **143**(1) 100 (1996)
[17] Zhong, Q., Bonakdarpour, A., Zhang, M., Gao, Y., & Dahn, J. R. *Journal of the Electrochemical Society*, **144**(1) 205 (1997)
[18] Takahashi, M., Yoshida, T., Ichikawa, A., Kitoh, K., Katsukawa, H., Zhang, Q., & Yoshio, M. *Electrochimica acta*, **51**(25) 5508-5514 (2006)
[19] Chemelewski, K. R., & Manthiram, A. *The Journal of Physical Chemistry C*, **117**(24) 12465-12471 (2013)
[20] Lee, Y. S., & Yoshio, M. *Electrochemical and Solid State Letters*, **4**(7) A85 (2001)
[21] Hernan, L., Morales, J., Sanchez, L., & Santos, J. *Solid State Ionics*, **118**(3-4) 179-185 (1999)
[22] Windmüller, A., Tsai, C. L., Möller, S., Balski, M., Sohn, Y. J., Uhlenbruck, S., & Guillon, O. *Journal of power sources*, **341** 122-129 (2017)
[23] Wang, S., Yang, J., Wu, X., Li, Y., Gong, Z., Wen, W., ... & Yang, Y. *Journal*

of Power Sources, **245** 570-578 (2014)
[24] Son, J. T., & Kim, H. G. *Journal of power sources*, **147**(1-2) 220-226 (2005)
[25] Feng, C., Li, H., Zhang, C., Guo, Z., Wu, H., & Tang, J. *Electrochimica acta*, **61** 87-93 (2012)
[26] Kang, Y. J., Kim, J. H., & Sun, Y. K. *Journal of power sources*, **146**(1-2) 237-240 (2005)
[27] Son, J. T., & Kim, H. G. *Journal of power sources*, **147**(1-2) 220-226 (2005)
[28] He, X., Li, J., Cai, Y., Wang, Y., Ying, J., Jiang, C., & Wan, C. *Solid State Ionics*, **176**(35-36) 2571-2576 (2005)
[29] Yonezawa, S., Yamasaki, M., & Takashima, M. *Journal of fluorine chemistry*, **125**(11) 1657-1661 (2004)
[30] Wen, W., Ju, B., Wang, X., Wu, C., Shu, H., & Yang, X. *Electrochimica Acta*, **147** 271-278 (2014)
[31] Jin, Y. C., & Duh, J. G. *ACS applied materials & interfaces*, ***8***(6) 3883-3891 (2016)
[32] Okumura, T., Fukutsuka, T., Matsumoto, K., Orikasa, Y., Arai, H., Ogumi, Z., & Uchimoto, Y. *Dalton transactions*, **40**(38) 9752-9764 (2011)
[33] Li, H., Luo, Y., Xie, J., Zhang, Q., & Yan, L. *Journal of Alloys and Compounds*, **639** 346-351 (2015)
[34] Du, G., NuLi, Y., Yang, J., & Wang, J. *Materials Research Bulletin*, **43**(12) 3607-3613 (2008)
[35] Feng, C., Li, H., Zhang, C., Guo, Z., Wu, H., & Tang, J. *Electrochimica acta*, **61** 87-93 (2012)
[36] Wang, M. S., Wang, J., Zhang, J., & Fan, L. Z. *Ionics*, **21**(1) 27-35 (2015)
[37] Xiong, L., Xu, Y., Tao, T., Song, J., & Goodenough, J. B. *Journal of Materials Chemistry*, **22**(47) 24563-24568 (2012)
[38] Li, P., Luo, S. H., Wang, J., Wang, X., Tian, Y., Li, H., ... & Liu, X. Preparation and electrochemical properties of Al-F co-doped spinel $LiMn_2O_4$ single-crystal material for lithium-ion battery. *International Journal of Energy Research*. (2021).